

Eliana M. Klier, Hongying Wang and J. Douglas Crawford

J Neurophysiol 89:2839-2853, 2003. doi:10.1152/jn.00763.2002

You might find this additional information useful...

This article cites 57 articles, 36 of which you can access free at:

<http://jn.physiology.org/cgi/content/full/89/5/2839#BIBL>

This article has been cited by 14 other HighWire hosted articles, the first 5 are:

Influence of Saccade Efference Copy on the Spatiotemporal Properties of Remapping: A Neural Network Study

G. P. Keith, G. Blohm and J. D. Crawford

J Neurophysiol, January 1, 2010; 103 (1): 117-139.

[\[Abstract\]](#) [\[Full Text\]](#) [\[PDF\]](#)

Kinematics of the Rotational Vestibuloocular Reflex: Role of the Cerebellum

M. F. Walker, J. Tian and D. S. Zee

J Neurophysiol, July 1, 2007; 98 (1): 295-302.

[\[Abstract\]](#) [\[Full Text\]](#) [\[PDF\]](#)

Three-Dimensional Eye-Head Coordination After Injection of Muscimol Into the Interstitial Nucleus of Cajal (INC)

F. Farshadmanesh, E. M. Klier, P. Chang, H. Wang and J. D. Crawford

J Neurophysiol, March 1, 2007; 97 (3): 2322-2338.

[\[Abstract\]](#) [\[Full Text\]](#) [\[PDF\]](#)

Interstitial Nucleus of Cajal Encodes Three-Dimensional Head Orientations in Fick-Like Coordinates

E. M. Klier, H. Wang and J. D. Crawford

J Neurophysiol, January 1, 2007; 97 (1): 604-617.

[\[Abstract\]](#) [\[Full Text\]](#) [\[PDF\]](#)

Head Movements Evoked by Electrical Stimulation in the Frontal Eye Field of the Monkey: Evidence for Independent Eye and Head Control

L. L. Chen

J Neurophysiol, June 1, 2006; 95 (6): 3528-3542.

[\[Abstract\]](#) [\[Full Text\]](#) [\[PDF\]](#)

Medline items on this article's topics can be found at <http://highwire.stanford.edu/lists/artbytopic.dtl> on the following topics:

Veterinary Science .. Superior Colliculus

Medicine .. Torsion

Medicine .. Eye Movement

Physiology .. Monkeys

Updated information and services including high-resolution figures, can be found at:

<http://jn.physiology.org/cgi/content/full/89/5/2839>

Additional material and information about *Journal of Neurophysiology* can be found at:

<http://www.the-aps.org/publications/jn>

This information is current as of March 22, 2010 .

Three-Dimensional Eye-Head Coordination Is Implemented Downstream From the Superior Colliculus

Eliana M. Klier, Hongying Wang, and J. Douglas Crawford

Canadian Institutes of Health Research Group for Action and Perception, York Centre for Vision Research and Departments of Psychology, Biology and Kinesiology and Health Sciences, York University, Toronto, Ontario M3J 1P3, Canada

Submitted 5 September 2002; accepted in final form 13 January 2003

Klier, Eliana M., Hongying Wang, and J. Douglas Crawford. Three-dimensional eye-head coordination is implemented downstream from the superior colliculus. *J Neurophysiol* 89: 2839–2853, 2003; 10.1152/jn.00763.2002. How the brain transforms two-dimensional visual signals into multi-dimensional motor commands, and subsequently how it constrains the redundant degrees of freedom, are fundamental problems in sensorimotor control. During fixations between gaze shifts, the redundant torsional degree of freedom is determined by various neural constraints. For example, the eye- and head-in-space are constrained by Donders' law, whereas the eye-in-head obeys Listing's law. However, where and how the brain implements these laws is not yet known. In this study, we show that eye and head movements, elicited by unilateral microstimulations of the superior colliculus (SC) in head-free monkeys, obey the same Donders' strategies observed in normal behavior (i.e., Listing's law for final eye positions and the Fick strategy for the head). Moreover, these evoked movements showed a pattern of three-dimensional eye-head coordination, consistent with normal behavior, where the eye is driven purposely out of Listing's plane during the saccade portion of the gaze shift in opposition to a subsequent torsional vestibuloocular reflex slow phase, such that the final net torsion at the end of each head-free gaze shift is zero. The required amount of saccade-related torsion was highly variable, depending on the initial position of the eye and head prior to a gaze shift and the size of the gaze shift, pointing to a neural basis of torsional control. Because these variable, context-appropriate torsional saccades were correctly elicited by fixed SC commands during head-free stimulations, this shows that the SC only encodes the horizontal and vertical components of gaze, leaving the complexity of torsional organization to downstream control systems. Thus we conclude that Listing's and Donders' laws of the eyes and head, and their three-dimensional coordination mechanisms, must be implemented after the SC.

INTRODUCTION

The output signal of the superior colliculus (SC) serves a basic physiological function—to re-direct the line of sight (Freedman et al. 1996; Klier et al. 2001; Roucoux et al. 1980). During natural head-free movements, these changes in gaze (i.e., eye-in-space) are accomplished through coordinated movements of both the eyes (i.e., eyes-in-head) and head (i.e., head-in-space) (Freedman and Sparks 1997; Guitton 1992; Phillips et al. 1995; Tomlinson 1990). But how are the initial visual signals transformed into the correct neural signals to

drive the muscles of the eyes and head? The images of objects in the environment are initially encoded in two-dimensional (2-D) retinal coordinates, whereas the neural signals sent to both the eye and neck muscles must be three-dimensional (3-D) in nature (Donders 1848; Richmond and Vidal 1998). The goal of the current study was to determine where and how, with respect to the SC, 2-D sensory signals are transformed into the appropriate 3-D motor commands for gaze shifts.

Our previous study (Klier et al. 2001) suggested that the SC encodes gaze commands in an eye-centered frame, but this is separate from the question of the SC's role in the 2- to 3-D visuomotor transformation. To understand the latter question, it is useful to briefly review the 3-D kinematics governing gaze shifts. Both the eyes and head can rotate about three mutually perpendicular axes: horizontal rotations about a vertical axis, vertical rotations about a horizontal axis, and torsional rotations about a naso-occipital axis (Fick 1854). However, any given desired gaze direction specifies only two of these variables (i.e., horizontal and vertical), leaving the torsional degree of freedom unspecified. This is a classic example of the degrees-of-freedom problem (Bernstein 1967; Crawford and Vilis 1995; Turvey 1990), which the brain solves in slightly different ways for the eyes and head.

Previous studies have shown that the eye-in-space (Es), the head-in-space (Hs), and the eye-in-head (Eh) each obey Donders' law, although to different degrees of precision (Glenn and Vilis 1992; Radau et al. 1994). Donders' law states that each gaze direction will be associated with only one, unique torsional value (Donders 1848). Specifically, the Eh obeys a form of Donders' law called Listing's law in which the torsional component at any gaze direction is held at zero in a head-fixed, orthogonal coordinate system named Listing's coordinates (Ferman et al. 1987; Helmholtz 1867; Tweed and Vilis 1990; Westheimer 1957). In contrast, the Es and Hs obey a different form of Donders' law in which torsion is minimized in Fick coordinates (i.e., where the orientation of an object relative to a chosen reference position is described by rotations in the following order: horizontal, vertical, torsional) (Crawford et al. 1999; Glenn and Vilis 1992; Medendorp et al. 1998; Misslisich et al. 1998; Radau et al. 1994; Theeuwes et al. 1993; Tweed et al. 1995). In the space-fixed orthogonal coordinate system used to measure these movements in most labs, this

Present address and address for reprint requests: E. M. Klier, Dept. of Anatomy and Neurobiology, 213 E. McDonnell SRF, Box 8108, Washington Univ. School of Medicine, 660 S. Euclid Ave., St. Louis, MO 63110 (E-mail: eliana@cabernet.wustl.edu).

The costs of publication of this article were defrayed in part by the payment of page charges. The article must therefore be hereby marked "advertisement" in accordance with 18 U.S.C. Section 1734 solely to indicate this fact.

results in clockwise (CW) values when gaze is directed up-left and down-right, and counterclockwise (CCW) values when gaze is directed up-right and down-left (Glenn and Vilis 1992; Radau et al. 1994). Of these rules, the Eh rule is obeyed most strictly (measured as torsional variance from the ideal zero torsion in Listing's coordinates), the Hs rule is obeyed less strictly, and Es rule, being the geometric outcome of the other two, is followed least strictly (Glenn and Vilis 1992; Radau et al. 1994).

Moreover, to be precise, Listing's law (of the Eh) is only observed when the head is motionless. Thus Listing's law, in some form or another, is obeyed at all times when the head is immobilized (Ferman et al. 1987; Tweed and Vilis 1990) and during fixations at the end of head-free gaze shifts (Crawford et al. 1999; Misslisch et al. 1998; Radau et al. 1994). But adherence to Listing's law is impossible *during* head-free gaze shifts. Here (Fig. 1), a target is acquired by a gaze shift (1), but then the head continues to move in approximately the same direction for some time (Freedman et al. 1996; Guitton and Volle 1987; Newlands et al. 2001). To stabilize the retinal image during this latter period (2), the vestibuloocular reflex (VOR) must rotate the Eh about an axis colinear with that of the Hs (Crawford and Vilis 1991; Misslisch and Hess 2000). If the head's axis of rotation has a torsional component, then the eye's axis must have an equal and opposite torsional component if the VOR is to be effective. This inevitably causes the Eh to break Listing's law, depending on initial eye position and the direction of head movement (Crawford and Vilis 1991; Crawford et al. 1999).

The potential cost of this for the system is that the Eh could end up with large torsional values at the end of the gaze shift, which would presumably result in both perceptual and motor problems for the gaze-control system (Crawford and Vilis 1991; Glenn and Vilis 1992; Radau et al. 1994; Tweed and Vilis 1990). These studies have proposed that Eh torsion is minimized to maintain lines parallel or perpendicular to the horizon and/or to minimize the energy output required by the eye muscles during fixations. Also, a recent study (Schreiber et al. 2001) found that the stereopsis system assumes that the normal Donders' laws are obeyed when matching points between the two eyes such that deviations from these laws disrupt depth vision.

To satisfy these two opposing goals (stabilizing the retinal image at the end of a gaze shift and landing final Eh positions in Listing's plane), the gaze-control system has developed a sophisticated coordination strategy (Crawford et al. 1999; Tweed et al. 1998). Rather than waiting for the VOR-related movement to drive the Eh out of Listing's plane, the system adds an equal but opposite amount of torsion to the Eh during the initial gaze shift. Thus Eh torsion is first driven out of Listing's plane during the gaze shift such that the following VOR-related head movement brings the Eh back into Listing's plane by the end of the head movement. This strategy has been shown in both humans (Tweed et al. 1998) and monkeys (Crawford et al. 1999). However, the physiological mechanisms of this 3-D coordination strategy, and other aspects of the implementation of Listing's and Donders' laws, have not yet been identified.

It is clear that the eye and head muscles themselves do not constrain torsion in the way required by Donders' law because these same muscles are known to produce large violations of

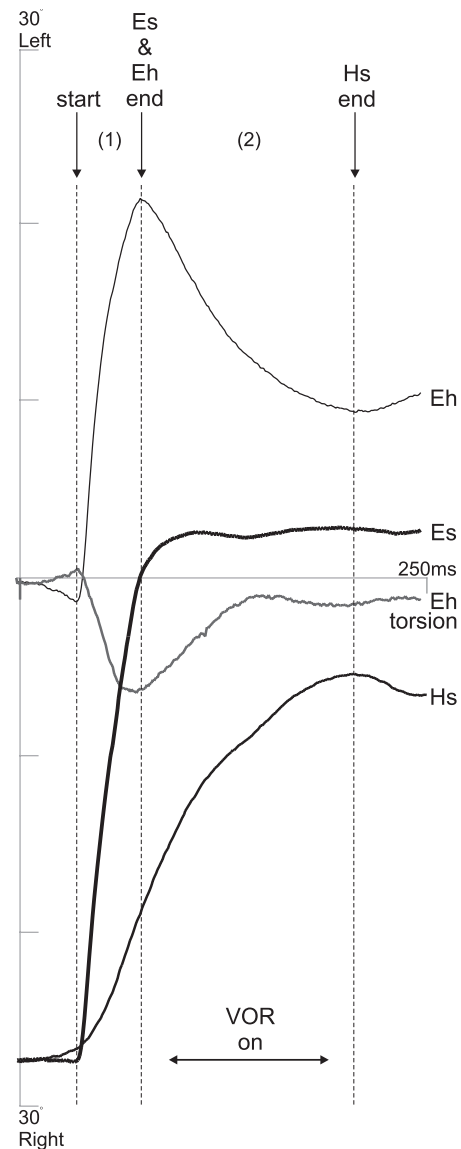


FIG. 1. A typical head-free gaze shift. Horizontal position traces of the eye-in-space (Es, dark trace), head-in-space (Hs, medium trace), and eye-in-head (Eh, light trace) are plotted as a function of time. All 3 variables start their movement at approximately the same time. The Es and Eh trajectories terminate first, and we refer to the time between movement onset and Es/Eh offset as the "gaze shift" (1). The Hs continues its movement after the Es/Eh end. We refer to this period as the VOR-related head movement (2) because the VOR must be active during this time to keep gaze (i.e., Es) fixed on the point of interest. A trace of torsional Eh position (gray) is also plotted to illustrate how torsion is built up during the gaze shift phase and then returns toward 0 during the VOR phase.

Donders' law under a variety of conditions (Ceylan et al. 2000; Crawford and Vilis 1991; Klier et al. 2002; Nakayama 1975). However, it is possible that the musculature is set up in some way that optimally suits the choice of implementation of Donders' law (Crawford and Guitton 1997; Demer et al. 1995; Quaia and Optican 1998). It has also been suggested that the innervation to the pulley system surrounding the extra-ocular muscles could change the position-dependent torsional torques produced by these muscles in ways to suit different 3-D oculomotor strategies (Demer et al. 2000). But even if it did, this system would still require a neural mechanism of some kind.

Thus the questions remain, where and how are the neural mechanisms for Donders' law implemented with respect to the SC?

One study has previously attempted to discern whether the SC outputs a 2- or 3-D gaze command. Van Opstal and colleagues (1991; also see Hepp et al., 1993) stimulated the SC in *head-fixed* monkeys and found that the Eh remained in Listing's plane throughout the entire stimulation-induced trajectory. From this they concluded that the SC outputs a 2-D signal. However, the interpretation of this result remains ambiguous. For example, this could mean that the SC outputs a 2-D signal to a Donders' law operator that determines the desired 3-D orientation of the Eh, or it could mean that the SC encodes horizontal and vertical components in parallel with a torsional controller. And of course, this head-fixed study tells us nothing of the role of the SC in implementing Donders' law of the Hs. To answer these questions, it is necessary to examine the role of the SC in implementing Donders' law during head-free gaze shifts.

Therefore to determine where the 3-D kinematics are added to the gaze-control signal, we compared 3-D aspects of normal head-free behavior with those of stimulation-induced, head-free behavior. If the 3-D kinematics are different in the two cases (i.e., if Donders' and Listing's laws are *not* obeyed during SC stimulations), then the 3-D restrictions are likely implemented upstream from or parallel to the SC. For example, if the SC implements a 2-D Eh command in parallel with a torsional controller, this would be adequate to provide Listing's law with the head fixed but not the sophisticated 3-D eye-head coordination strategy observed with the head free. Conversely, if Donders' laws of the Eh and Hs are obeyed equally well in both conditions (in terms of both the type of rule and the degree of precision to which it is followed, including the normal mechanisms for 3-D eye-head coordination), then their implementations must occur downstream from the SC.

METHODS

Surgery and equipment

Two monkeys (*Macaca fascicularis*) underwent aseptic surgery under general anesthesia (isoflurane, 0.8–1.2%) during which they were each fitted with an acrylic skull-cap, a stainless steel chamber (centered at 5 mm anterior and 0 mm lateral in stereotaxic coordinates) that allowed access to the brain, and a stainless steel cylinder, used in combination with a bolt and screw, to immobilize the head when required. 3-D eye movement recordings were made possible by implanting two 5-mm-diam scleral search coils in the right eye of each animal (one coil was placed in the nasal-superior quadrant, while the 2nd was located in the nasal-inferior quadrant such that the two were not parallel). 3-D head movements were recorded via two orthogonal coils screwed to a plastic platform on the skull-cap during experiments. Animals were given analgesic medication and prophylactic antibiotic treatment during the post surgical period, and experiments commenced after 2 wk of postoperative care. These protocols were in accordance with Canadian Council on Animal Care guidelines on the use of laboratory animals and preapproved by the York University Animal Care Committee.

The primate chair was placed such that each monkey's head was at the center of three mutually orthogonal magnetic fields (90, 125, and 250 kHz.), each 1 m in diameter. Prior to each experiment, these fields were calibrated for both the eye and head coils using a homemade

gimbal that allowed for torsional, vertical, and horizontal rotations. This plexiglass gimbal was placed in the center of the three fields and an eye coil (similar to the one implanted in the monkey's eye) was fixed to the center of the gimbal. The gimbal was then rotated so that the coil was perpendicular with one of the three fields. In this position, a maximum signal is generated in the coil by the orthogonal magnetic field. The gain and bias were then adjusted such that this maximum signal was 8 V. This procedure was repeated in all three magnetic fields with the eye coil and then again with the head coil (the same head coil that would later be fixed to the monkey's head).

This calibration procedure assumes that the eye and head coil used for calibration are identical to those used by the monkey during experimentation. This assumption is true for the head coil. Although the eye coil used for calibration was not the same one used during experimentation, the calibration coil did come from a batch of homemade eye coils that would otherwise have been implanted. Thus its construction was identical to the coil found in the monkey. Also, periodic impedance checks of both the implanted and calibration coils further assured us that the two were comparable. A second assumption involves the stability of the signal being generated by the magnetic fields. Over many years of using our fields and similar ones like it, it is recommended that, once turned on, the fields be given ~1-h to warm up and obtain a steady output signal. Thus our calibration procedure only began once this 1-h period has passed. Finally, our procedure requires that the magnetic fields be consistent within the range of movement occupied by the eye and head. A previous analysis found that coil systems such as our own are accurate to $\leq 2\%$ (magnitude)/ $\leq 2.05^\circ$ (direction) within a ± 10 -cm radius from center (where the calibration occurs) (Klier et al., 1998). Because neither the eyes nor the head either rotate or translate out of that range, we are confident in the recorded measures.

During each experiment, the monkey sat in a modified Crist Instruments primate chair such that its head and neck were free to move as desired. Specifically, the top plate was removed and replaced by canvas cloth that buckled snugly at the back, similar to the system used by Freedman and Sparks (1997). The upper body (to the shoulders) was prevented from rotating in the yaw direction (i.e., movement around an earth-vertical axis) by the use of plastic molding over the shoulders. *Monkey 1 (M1)* also wore a primate jacket (Lomir Biomedical) that further secured the upper body to the chair with restraints, whereas *monkey 2 (M2)* was solely held by additional plastic molding sculpted to the dorsal upper torso. These different restraining techniques may have given M2 more freedom of movement in the upper body than M1.

Experimental procedures

At the beginning of each experiment, with the head fixed, a tungsten micro-electrode (FHC; 0.5–1.5 M Ω impedance) was slowly lowered down a preselected track with the use of a hydraulic micro-drive (Narishige model MO-99S). Neuronal activity was output on an audio monitor. We first identified burst-tonic neurons in the interstitial nucleus of Cajal (INC) as a landmark (Klier et al. 2002) and subsequently moved our electrodes posteriorly to the stereotaxic coordinates corresponding to the SC. If burst activity was heard along with corresponding contralateral eye movements, then the site was deemed to be a potential SC site. Potential SC sites were further confirmed by observing eye movements elicited after head-fixed stimulation. If conjugate contralateral eye movements were elicited via stimulation, then we classified the site as an SC site.

With the head free, the electrode would then be lowered through the same track in which head-fixed recording and stimulation indicated SC activity. Every 0.5 mm stimulations of 50 μ A with pulse widths of 0.5 ms (300 Hz), and pulse trains of 200 ms (500 Hz) were delivered automatically every 3.3 s (via Grass Instruments model S88) in both dim light and in the dark. Such train durations have been shown to produce maximum site-specific gaze amplitudes without saturation

(Freedman et al. 1996). In addition, these stimulation patterns are thought to emulate a fairly realistic pattern of spatial activity in the SC (Munoz and Wurtz 1995) and are known to evoke natural-looking 2-D patterns of eye-head coordination in the monkey (Freedman et al. 1996; Klier et al. 2001). Pulse trains of 100, 300, 400, and 500 ms were also delivered; however, these data are not included in this paper. During experimentation, the eye and head coils were viewed on-line in an adjacent room as well as recorded at 500 Hz for further off-line analysis (see Tweed et al. 1990).

The monkeys were untrained with regard to making gaze shifts and were never required to make saccades with the head-fixed for extended periods of time. As the stimulations were delivered, the monkeys simply moved their eyes and heads freely and naturally. Some of these movements were self-initiated, while others were encouraged. One experimenter always stood hidden behind a hemi-spherical dome [barrier paradigm (Guitton et al. 1990)] and motivated the monkeys to use their entire eye/head motor ranges by presenting the monkeys novel visual objects (in dim light) and novel sounds (in the dark). A second experimenter viewed the eye/head movements on-line and provided verbal feedback about the range of initial positions obtained. This was done to obtain the large range of initial eye and head positions necessary for the surface fits described in the following text (see *Surface fits*).

As a control to the SC stimulation data, a "random" control paradigm was run at the beginning of each head-free experiment. In this paradigm, the monkeys were again required to look around freely and encouraged to maximize their ocular and head motor ranges in the same way described in the preceding text. However, no stimulations were delivered during these controls.

Of a total of 77 putative sites tested, 51 qualified to be included in this paper on the basis of two criteria: gaze shifts were consistently evoked during all stimulations and movements of both the eye and head were evoked. In practice, these two factors were associated. Rejected sites tended to lie on the fringes and more superficial sites of the SC. In M1, 13 sites were examined in the right SC and 2 sites in the left SC. In M2, 20 sites were investigated in the right SC and 16 sites in the left SC.

Data analysis

QUANTIFICATION OF COIL SIGNALS. At the beginning of each head-free experiment, each monkey was required to fixate its own image, for 5–10 s, in a 5 × 3-cm mirror. The mirror was located 0.75 m directly in front of the monkey's head, and thus gaze was oriented directly straight ahead along the forward pointing magnetic field. This measure of straight ahead was sufficiently accurate for quantitative comparisons between controls and data recorded within a given experiment. Coil signals were measured at this position and were used as the initial reference position for the eye and head in space coordinates. This reference position was then used to compute quaternions using a method described previously (Tweed et al. 1990). The quaternions were also transformed into linear angular measures of 3-D eye position (Crawford and Guitton 1997) for statistical analysis. In this way, any final eye orientation could be described as a rotation vector from the initial reference eye position. The torsional thickness (quantified as the torsional SD) of these data were computed using the algorithm described in Tweed et al. (1990).

COORDINATE SYSTEMS. The raw eye/head coil data were initially represented in an earth-fixed orthogonal coordinate system defined by the magnetic fields that we called "space" coordinates. Quaternions calculated from these signals represented eye/head orientations in space (Es/Hs). Eye-in-head (Eh) orientations were computed from both the eye and head coil signals by dividing the Es quaternion by the Hs quaternion (Glenn and Vilis 1992) as follows

$$Eh = Es(Hs)^{-1}$$

To put the Eh data into Listing's coordinates, quaternions derived from "planes of best fit" (see following text) were used to rotate space coordinates to align with Listing's plane (Tweed et al. 1990). An analogous process was sometimes used to view Es and Hs data "edge-on" against the torsional axis. Finally, Hs rotations were sometimes rotated into Listing's coordinates (of the eye) for comparison with the VOR, as described in Fig. 11 of RESULTS.

SURFACE FITS. To quantify the orientation ranges of Es, Hs, and Eh, second-order surface fits were made to Es, Hs, and Eh quaternions using a procedure described previously (Glenn and Vilis 1992; Radau et al. 1994; Tweed et al. 1990). Second-order fits were chosen over first- or third-order fits because they have been shown to provide the most useful description of similar primate data without becoming overly complex (Crawford et al. 1999; Glenn and Vilis 1992; Radau et al. 1994). The following formula provides the equation for a second-order fit for a generic position quaternion (q) where $q = q_0 + q_1 + q_2 + q_3$

$$q_1 = a_1 + a_2q_2 + a_3q_3 + a_4(q_2)^2 + a_5q_2q_3 + a_6(q_3)^2$$

This is a 3-D description of torsional position (q_1) as a function of various combinations of vertical (q_2) and horizontal (q_3) positions (fit coefficients a_1 – a_6). Once such a 2-D "surface of best fit" has been computed, the SD of the torsional components of all actual positions from this fit can be computed using the method described in Tweed et al. (1990).

Because we observed the same pattern of eye-head coordination reported in virtually every other head-free study (Freedman and Sparks 1997; Guitton 1992; Phillips et al. 1995; Tomlinson 1990), we subdivided combined eye/head gaze shifts into two parts (Fig. 1): a gaze movement, involving both the Eh and Hs, that brings the line-of-sight (Es) onto the target first and a continuation of the lagging Hs movement that brings the Eh toward the center of the orbits. The latter is accompanied by the VOR, which drives the Eh in an equal and opposite direction to that of the Hs. Thus the Es and Eh remain on target until the Hs stops its movement.

The preceding measures of fit and variance were applied to the following subranges of the data. The "fixation" range was defined to be those positions where the velocity of both the Es and Hs were $<10^\circ/s$. The "end of gaze" range indicates positions at the end of the Es movement (i.e., when gaze reaches its new position). The "end of head" range specifies the positions at which the head stopped its movement (i.e., at the end of the VOR-related movement). Algorithms were used to compute these measures in controls (i.e., the random paradigm) where the data are known to follow stereotypical velocity-position rules (Crawford et al. 1999). However, with the stimulation data, the latter two position ranges were chosen manually from quaternion versus time traces of Es, Hs, and Eh because this method was found to be more reliable than automatic selection software.

COMPUTING THE CHARACTERISTIC VECTOR. The characteristic vector for each stimulation site represents the theoretical movement trajectory that would be elicited at a given site if the monkey is looking straight ahead (i.e., 0° torsional, 0° horizontal, 0° vertical) when the stimulation train is delivered. Individual characteristic vectors for the Es, Hs, and the Eh can be obtained by selecting the 3-D starting and ending points of the eye and head trajectories, computing the displacement of each movement in the torsional, vertical, and horizontal dimensions, and performing a multiple linear regression on the stimulation-induced displacements of Es, Hs, and Eh as a function of their initial starting positions. This calculation, which takes into account between 30 and 60 stimulations per site, results in three vectors (Es, Hs, and Eh), which have their tail ends at the origin and extend to the site-specific amplitude. This analysis was done so that we could compare the stimulation-induced movements across different SC sites.

RESULTS

Control data

Before one can evaluate the 3-D aspects of SC stimulation-induced movements of the eyes and head, it is necessary to be familiar with the 3-D characteristics of normal head-free behavior. Figure 2 shows typical ranges of the Es (*top*), Hs (*middle*), and Eh (*bottom*) during the random paradigm. Each fixation position is represented as the tip of the rotation vector necessary to take the eye/head from its reference position to its current position. The data for these three variables are plotted according to the right-hand rule (the right thumb, aligned with the origin and any one point, specifies the rotation axis used, and the fingers of the right hand curl in the direction of motion). The *left* (A–C) is a view from behind the animal in which vertical versus horizontal components are plotted, whereas the *middle* (D–F) and *right* (G–I) columns show a side view in which torsional versus horizontal components are shown. Plotted in the *left* and *middle* are the tips of 3-D rotation vectors (i.e., quaternions) during gaze fixations, whereas in the *right*, 2-D best-fit surfaces to the corresponding quaternions in the *middle* are shown.

As one can see, the animals typically obtained a wide range

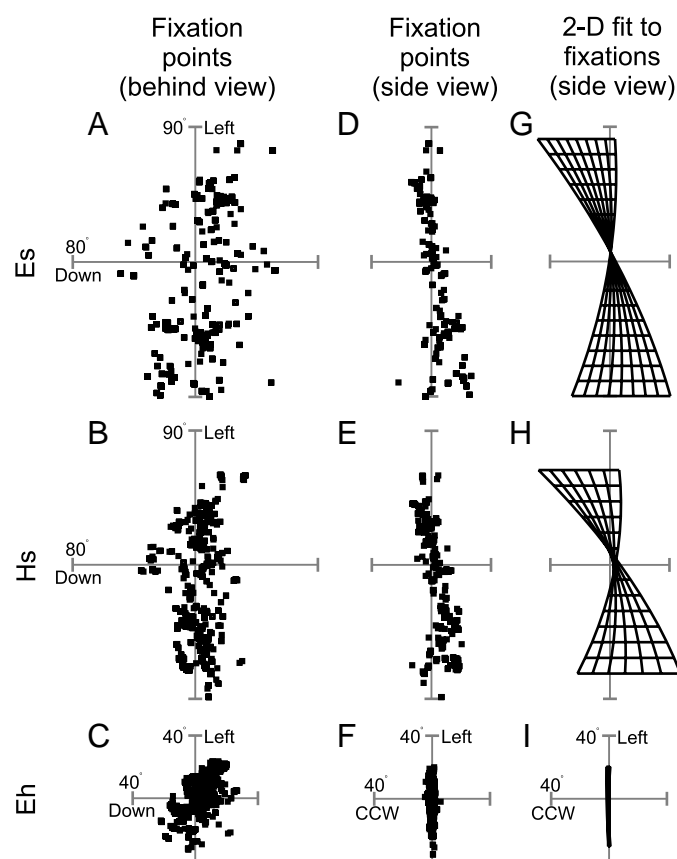


FIG. 2. Normal 3-dimensional (3-D) head-free behavior. A–C: fixation points (i.e., when the velocity of both the eye and head were $<10^\circ/\text{s}$) of the Eh, Hs, and Es taken from random gaze shifts are plotted from behind (■). D–F: data from *left* shown in a side view where torsion is plotted along the abscissa. G–I: 2nd-order best-fit surfaces were computed to the data in *middle*. The Eh surface appears to be a flat plane viewed edge-on, while the Hs and Es look like flat planes twisted about the center. Determining how well Listing's and Donders' laws are obeyed is measured by how well the points in *middle* adhere to their best-fit surfaces in *right* (see text for values).

of horizontal and vertical positions throughout the ocular and head motor ranges. As shown previously (Crawford et al. 1999; Glenn and Vilis 1992), the Hs tended to contribute more to horizontal positions than the Eh. In the *middle*, it is clear that the fixation ranges are restricted along the torsional axis. The Eh range seems to be most restricted as the data gathers around 0° on the abscissa. In other words, the Eh fixation points appear to align with Listing's plane, which, in this case, happens to align with the ordinate. In comparison, the Hs and Es seem somewhat less restricted yet still confined to a region relatively close to zero torsion. However, this observation cannot be objectively evaluated until the 3-D shape of these ranges is quantified.

To better visualize these restricted position ranges, we generated best-fit surfaces to the data in the *middle*. Here (*right*), one can recognize the characteristic surfaces (Glenn and Vilis 1992; Radau et al. 1994). The Eh produced a flat, planar surface that is viewed edge-on. In contrast, the Hs and Es produced twisted planes resembling bow-ties when viewed edge-on. This particular twist indicates that torsion was incurred in a clockwise direction at up-left and down-right gaze positions and in a counterclockwise direction at up-right and down-left gaze positions, in Listing's coordinates. As described in detail elsewhere (Crawford et al. 1999), these resultant surfaces are highly consistent across experiments and across monkeys.

As a quantitative measure, it is important to know how well the computed position quaternions (fixation points in *middle*) adhere to these 2-D surfaces (*right*). This is computed through a measure called "torsional SD" (Tsd) in which the scatter of the data relative to the fitted surface is defined by the SD of the distances of all the data points, in the torsional direction, relative to the fitted surface. If the Tsd is small, then the points adhere to their best-fit surface well and Donders' law is obeyed. If the Tsd is large, then torsion is not being tightly constrained and thus Donders' law is not being obeyed. Previous 3-D, head-free experiments in humans have found Tsd's in the range of $2\text{--}4^\circ$ for the Es, $2\text{--}5^\circ$ for the Hs, and $1\text{--}5^\circ$ for the Eh (Glenn and Vilis 1992; Radau et al. 1994). Similar analyses in monkeys have found Tsd's of the Es to be between 4.0 and 4.5° , 3.5 and 4.0° for the Hs and 1 and 3° for the Eh (Crawford et al. 1999). Although these ranges are somewhat variable and although there is no well-defined threshold regarding Tsd and Donders' law, these ranges differ greatly from the much larger, and sometimes purely, torsional violations observed in the Es, Hs, and Eh when stimulating brain stem centers, such as the interstitial nucleus of Cajal, which clearly do not obey Donders' law (Crawford and Vilis 1991; Klier et al. 2002).

Averaged across all random trials, the Tsd's (in degrees) were 3.27 ± 0.58 (Es), 3.09 ± 0.46 (Hs), 1.21 ± 0.06 (Eh) for M1 and 6.43 ± 0.50 (Es), 6.50 ± 0.69 (Hs), 1.70 ± 0.18 (Eh) for M2 (means \pm SE). These results are similar to previously reported findings in monkeys (Crawford et al. 1999) and in humans (Glenn and Vilis 1992; Radau et al. 1994) except that the Tsd for the Hs (and consequently the Es) for M2 was consistently higher than typical. The important question here, however, is whether these same patterns are preserved during stimulation of the SC.

Stimulus-evoked gaze shifts

Typical results of stimulating one site in the right SC of one monkey are shown in Fig. 3. The top row depicts stimulation-induced movements and endpoints (○) from a behind view (vertical vs. horizontal), whereas the bottom row shows the same data from a side view (torsion vs. horizontal). These endpoints were selected independently for the Es/Eh (i.e., at the end of the gaze shift) and the Hs (i.e., at the end of the head movement). The Es trajectories, whose kinematics are a product of the Hs and Eh trajectories till the end of the gaze shift, are plotted in Fig. 3A. Again, a wide range of initial Es positions was obtained to derive as-accurate-as-possible surface fits to the range of endpoints and to reveal any position dependencies in the resulting kinematics. It is noteworthy that these movements were rather convergent and not fixed vector movements. This was expected, especially for such large-amplitude gaze shifts, because of the retinotopic coding used by structure (Klier et al. 2001). The Hs trajectories (B) moved in the same direction as the Es, but their size was consistently smaller. Finally, the Eh (C and D) exhibited the most convergent movements and the narrowest overall range. Note that during the gaze shift (C), the Eh was initially driven out toward a peripheral point. However, after the Es trajectory had ended,

but the head was still moving (D), the Eh was driven back toward center.

From a 3-D perspective (side views), the trajectories of all three variables appeared to be constrained torsionally as during normal behavior. The Eh (G and H) movements seemed to be most tightly constrained, whereas the Es (E) and Hs (F) appeared to have more freedom in the torsional dimension. Specifically for the Eh, there was a fanning-out pattern of movement during the gaze shift (G) that was subsequently followed by re-centering torsional trajectories that drove the Eh back to Listing's plane (H). Thus the VOR slow phases tended to re-center the Es in all three dimensions.

To document these observations across all the SC stimulation data, we first calculated the "characteristic vector" for each stimulation site (see METHODS). Figure 4 shows the tips of these characteristic vectors for *M1* (●) and *M2* (○) for Es, Hs, and Eh (from gaze onset to gaze offset and from gaze end to head end). The behind views (A–D) show the variety of SC sites stimulated. The large range of horizontally induced movements indicates that many sites distributed along the rostral-caudal pole of the SC were stimulated, whereas the vertical range indicates that sites along the medial-lateral pole were also examined. The Eh plots (C and D) show that while the stim-

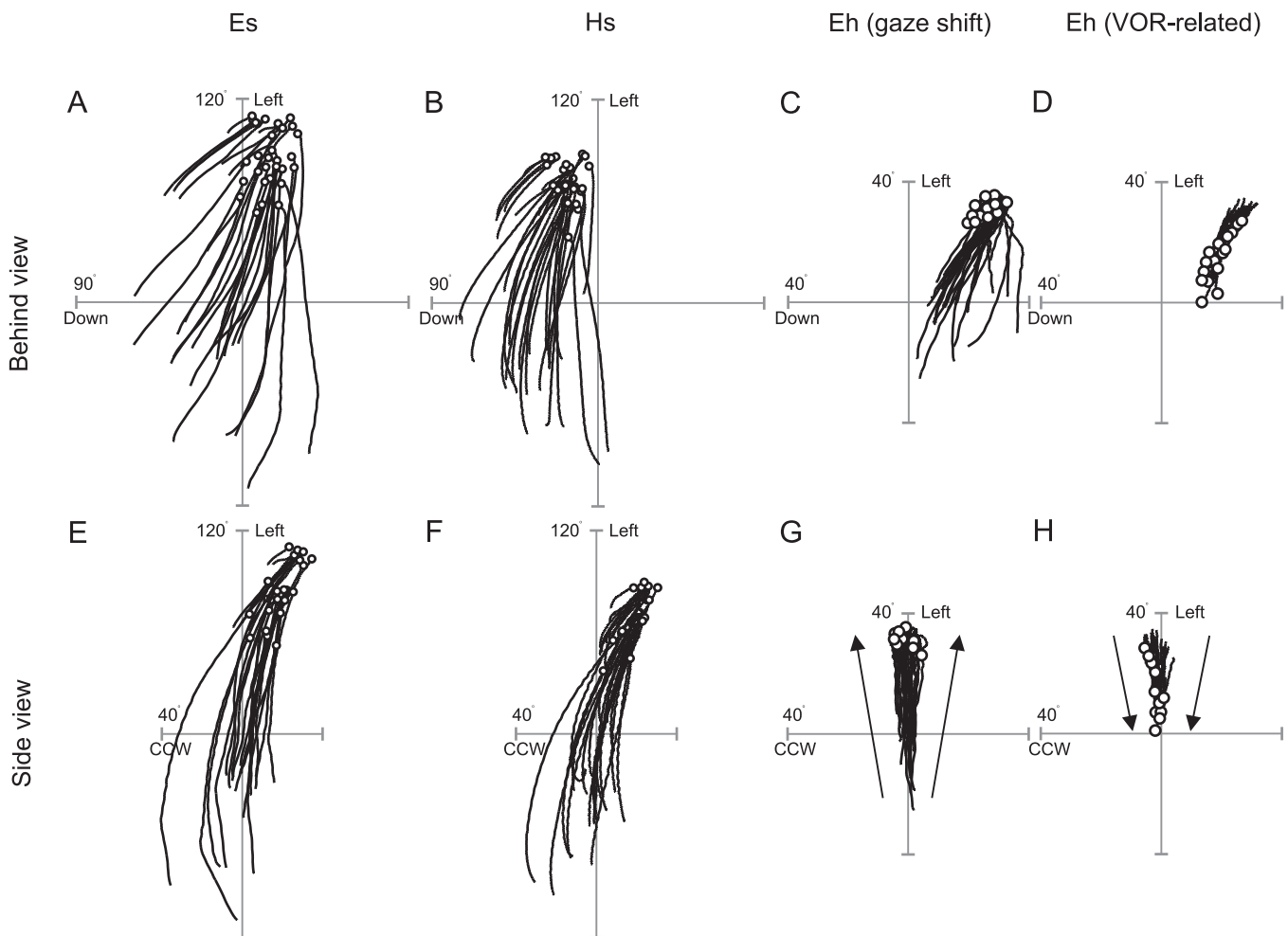


FIG. 3. Es, Hs, and Eh movements evoked by superior colliculus (SC) stimulation. A–D: behind views of resultant trajectories, where ○, final landing positions. E–H: side views of the corresponding data from *far left* where torsion is plotted along the abscissa. →, the overall pattern of Eh torsional movements.

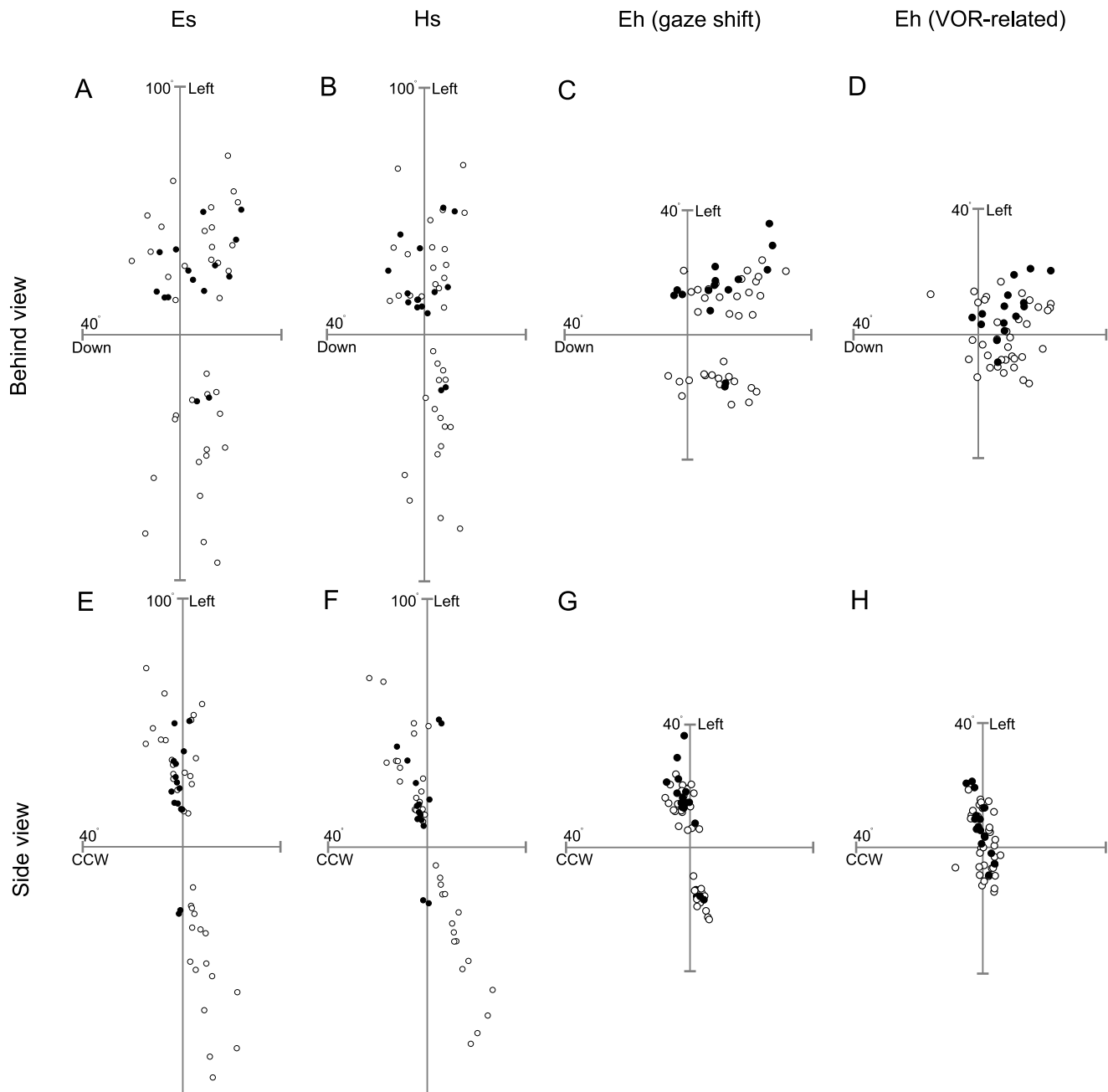


FIG. 4. Stimulation-induced characteristic vectors. Each point represents the predicted endpoint of stimulation-induced movement from 1 site in the SC if initial eye and head positions were at 0° torsion, 0° vertical, and 0° horizontal in space coordinates. Data are shown for M1 (●) and M2 (○). A–D: behind view of the Es, Hs, and Eh. E–H: side view of Es, Hs, and Eh.

ulations drove the Eh to various eccentric horizontal/vertical positions, the subsequent VOR-related head movements had a re-centering effect (i.e., the 2 distinct subgroups in C—1 from left SC sites and 1 from right SC sites—become 1 indistinguishable group in D).

The side views (E–H) highlight the torsional restrictions placed on these data. Although all three variables had reduced torsional ranges, the Eh was most limited, followed by the Hs and Es. This is in marked contrast to movements evoked by stimulation of motor sites further downstream such as the interstitial nucleus of Cajal, which produces much larger torsional rotations of both the eyes and head (Crawford et al. 1991; Klier et al. 2002). Finally,

note that the amount of Eh torsion appeared to decrease between the end of the gaze shift and the end of the head movement (again, the 2 distinct groups in G become 1 unified group in H). This shows that the VOR centering effect occurred in all three dimensions. Thus stimulation of the SC evokes movements which, at first glance, might seem to obey Donders' law. But, to settle this question, a more quantitative comparison of the control and stimulation data are required.

Comparing shapes of the Donders' surfaces

One way to see if the stimulus evoked movements obeyed Donders' law is to compare the shape of the stimulation-

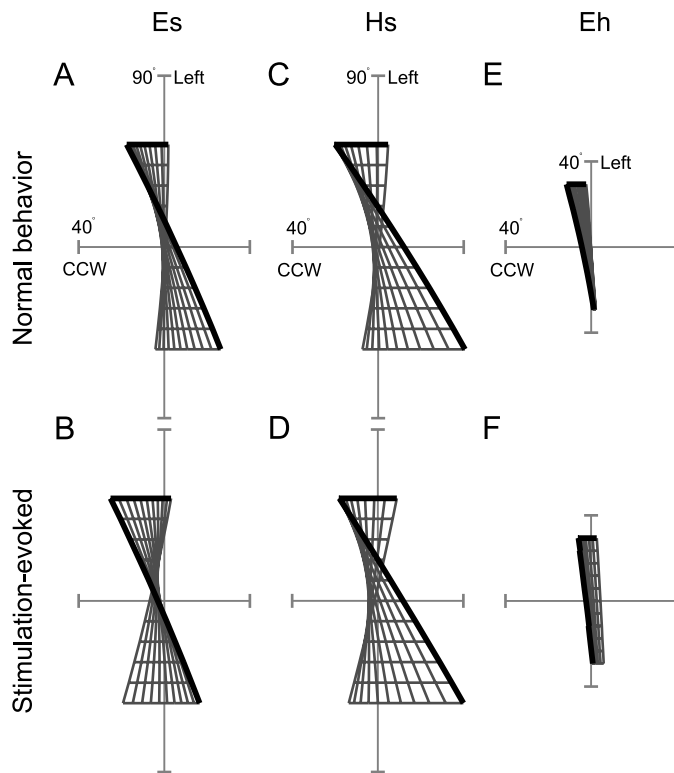


FIG. 5. Best-fit surfaces from control vs. SC stimulation-induced data. The 6 variables describing 2nd-order best-fit surfaces to the endpoints of control (*top*) and SC stimulation-induced (*bottom*) data were averaged across all random files (control data) and all sites tested (SC stimulation data). The 6 averaged variables produced 2nd-order surfaces which are shown from a side view (torsion along the abscissa). The resultant planes can be compared for the Es (A and B), Hs (C and D), and Eh (E and F). Statistical analysis (see text) showed that the corresponding surfaces were not significantly different from one another.

induced ranges to those of the controls. Unfortunately, the horizontal-vertical range of the endpoints for a given stimulation site was not generally large enough (Fig. 3) to provide the complete Donders' surface as obtained from controls (Fig. 2). This is because stimulating any one SC site, say in the right SC, only produces leftward movements that terminate in the left quadrant relative to space and/or the head. Therefore this comparison was made by treating the stimulation data as a population and then comparing its averaged data to controls. This was done by obtaining the fit coefficients (parameters a_1 – a_6) describing the Es, Hs, and Eh planes from each stimulation site. (Note that here the Es end points were taken at the end of the head/VOR movement.) We then averaged these a values to obtain an overall illustration of the stimulation-induced surface. These averaged surfaces are shown in Fig. 5, B, D, and F. For comparison, we averaged the a values derived from the random trials (i.e., those describing normal, head-free behavior) and plotted the results in Fig. 5, A, C, and E. Comparing the panels down each column, one can see that the surfaces obtained from normal, head-free behavior look nearly identical to the surfaces derived from stimulation-induced movements. The ranges seem to share similar twists, curvatures, tilts, and offsets.

To quantify this, we conducted statistical analyses (t -test with Bonferroni family-wise corrections, $P = 0.008$) on the a values that were obtained across the stimulation sites and

compared them to the a values obtained from control behavior (random trials). These comparisons were made for a values of the Es, Hs, and Eh for each of the two monkeys. For both *M1* and *M2*, the six a values for each of the three variables (Eh, Hs, and Es) were never significantly different from one another (lowest $P = 0.31$). These comparisons were made using the dim stimulation condition because the random trials were conducted in dim light, however, the averaged a values from the dark condition were also not significantly different from controls (lowest $P = 0.28$).

Adherence of stimulation end points to ideal Donders' surfaces

The previous section showed that there is no significant difference between the ideal Donders' surfaces fit to the control and stimulation data, perhaps suggesting that these data in fact adhere to the same Donders' rules. If so, then the stimulation end points should adhere to the ideal surface fits of the control data with the same degree of precision as the control data they were initially derived from.

Figure 6 shows the end points of SC stimulation for three

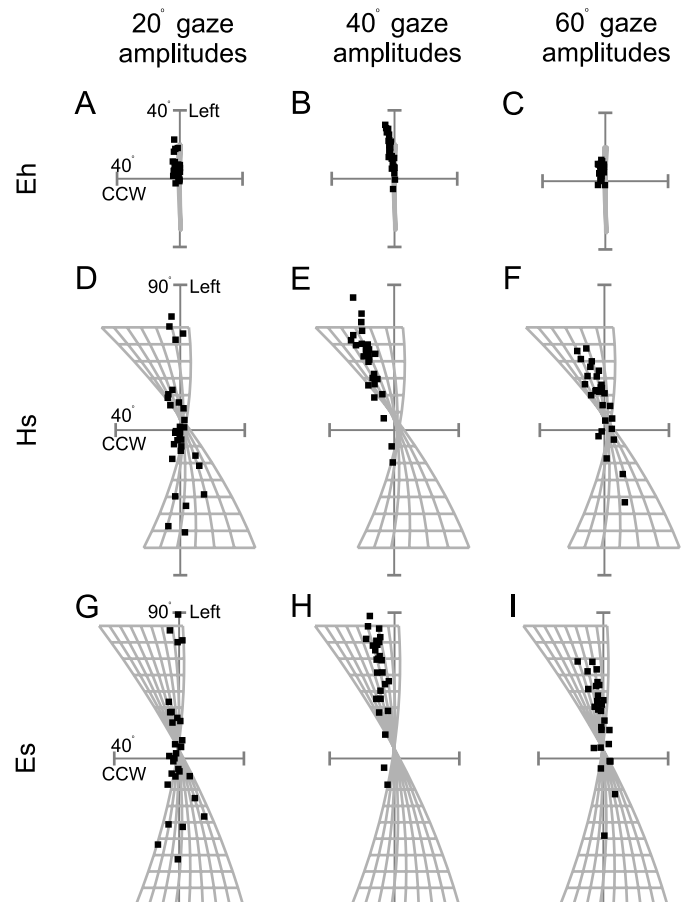


FIG. 6. SC stimulation-induced endpoints from 3 SC sites. A–C: side views of Eh endpoints (■) derived from stimulating 3 SC sites encoding movements with gaze amplitudes of $\sim 20^\circ$, 40° , and 60° , respectively. Best-fit surfaces from control data are shown in the background for comparison. D–F: corresponding data for Hs. G–I: corresponding data for Es. How well Listing's and Donders' laws are obeyed by the stimulation-induced data can be evaluated by computing how well the endpoints adhere to their corresponding best-fit surfaces (see text for values).

different sites in the right SC of one monkey. The stimulation endpoints (■) are shown for the Eh (*top*), the Hs (*middle*), and the Es at the end of the head/VOR movement (*bottom*). These points are superimposed on the corresponding second-order, best-fit surfaces made to the control data (from Fig. 2, *G–I*). On initial inspection, at the end of all SC stimulation-induced movements, the Eh endpoints seem to land on Listing's plane, while the Hs and Es end points appear to terminate within the range described by the twisted Donders' surfaces.

However, this comparison is made difficult by the fact that the Donders' surfaces are not generally flat or viewed edge on. Therefore we re-calculated the stimulation endpoint data in Listing's coordinates for the Eh (because Eh data are known to obey Listing's law) and in Donders' coordinates for the Hs and Es (i.e., with the same horizontal and vertical components but with torsion measured relative to the ideal control Donders' surfaces that the Hs and Es adhere to). These plots are shown in Fig. 7. Notice that now the Eh, Hs, and Es end points (■) are much more closely grouped about zero torsion.

To quantify this observation, the Tsd's of the random endpoints were first calculated (relative to the planes derived from control data; Fig. 8). On average the random Tsd's (in degrees) were 1.74 ± 0.13 (Eh), 4.68 ± 0.37 (Hs), 4.37 ± 0.48 (Es) for *M1* (*top left*) and 2.15 ± 0.10 (Eh), 7.59 ± 0.43 (Hs), $7.21 \pm$

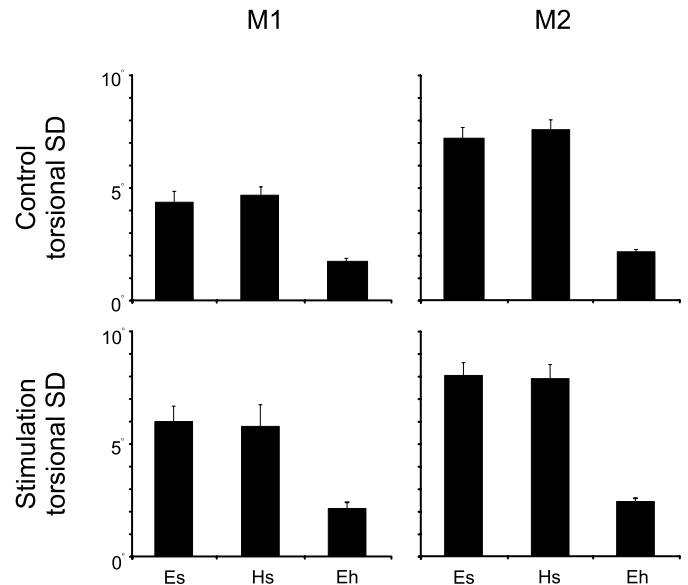


FIG. 8. Torsional SDs (Tsd) of Es, Hs and Eh at the end of the control (*top*) and stimulation-induced (*bottom*) movements for *M1* (*left*) and *M2* (*right*). In both conditions (control vs. stimulation), the Tsd at the end of the movements was comparable within each animal (see text for values).

0.48 (Es) for *M2* (*top right*). They were then compared with the Tsd of the stimulation-induced end points (*bottom*). On average the stimulation Tsd's (in degrees), in the comparable dim light condition, were 2.14 ± 0.28 (Eh), 5.79 ± 0.96 (Hs), 6.00 ± 0.68 (Es) for *M1* and 2.44 ± 0.15 (Eh), 7.91 ± 0.63 (Hs), 8.05 ± 0.57 (Es) for *M2*. When *t*-test (with Bonferroni family-wise corrections, $P = 0.017$) were performed across all stimulation sites, for both animals, there were no significant differences in Tsd between the two conditions (random vs. stimulation) for the Eh ($P = 0.43$, *M1*; $P = 0.50$, *M2*), Hs ($P = 0.53$, *M1*; $P = 0.86$, *M2*), or Es ($P = 0.20$, *M1*; $P = 0.60$, *M2*). These comparisons were made using data from the dim stimulation condition; however, similar comparisons made with data from the dark stimulation condition produced comparable results (for all 3 variables, in both monkeys, all P values > 0.05). Thus the stimulation end points terminated in a 3-D area indistinguishable from that produced by end points elicited during normal, head-free behavior. This shows that whatever mechanisms are used to control the torsional degree of freedom for the eye and head, they are accessed equally well by fixed stimulations to the SC as by naturally evoked gaze shifts.

Head-fixed versus head-free

In a previous study, van Opstal et al. (1991) showed that when the SC is stimulated with the head fixed, Eh trajectories remain in Listing's plane throughout the entire movement. Our head-fixed results showed the same pattern. Figure 9, *A* and *B*, illustrates torsional, vertical, and horizontal components of Eh saccades made with the head fixed. Figure 9*A* shows a spontaneous saccade, whereas Fig. 9*B* shows SC stimulation-evoked trajectories (these examples were matched for direction and amplitude). In both cases, the Eh was driven leftward and upward, but notice that the torsional component remained at 0° , in Listing's coordinates (abscissa), throughout the entire movement. But what happens when the head is free to move?

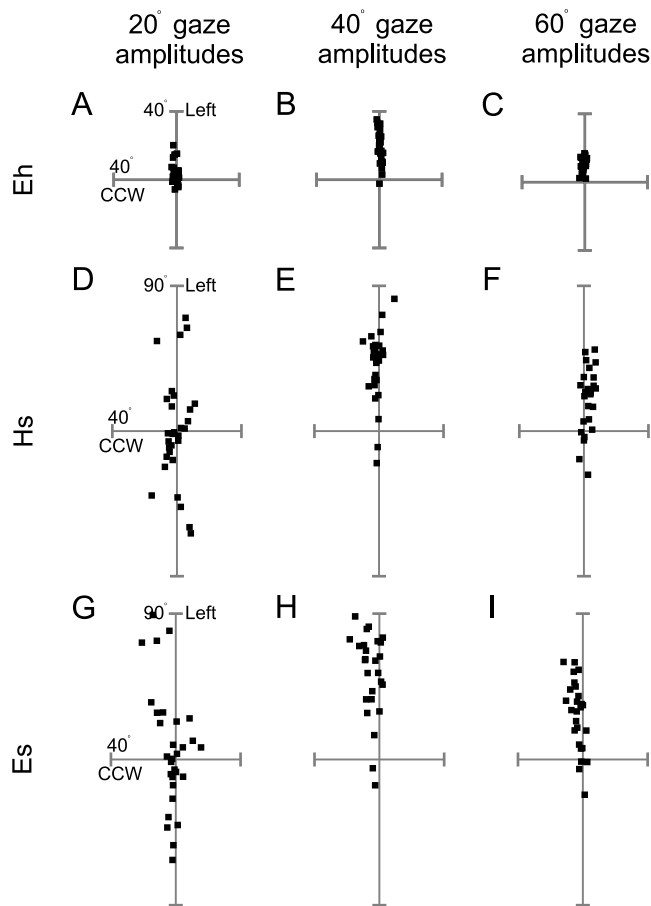


FIG. 7. SC stimulation-induced end points from Fig. 6 plotted in their appropriate coordinate systems. *A–C*: side views of Eh endpoints (■) in Listing's coordinates. *D–F*: Hs end points in Donders' coordinates. *G–I*: Es end points in Donders' coordinates. Note that although the data points seem to gather more closely around 0° torsion for larger amplitude movements of the Es and Hs, such a trend was not found across sites.

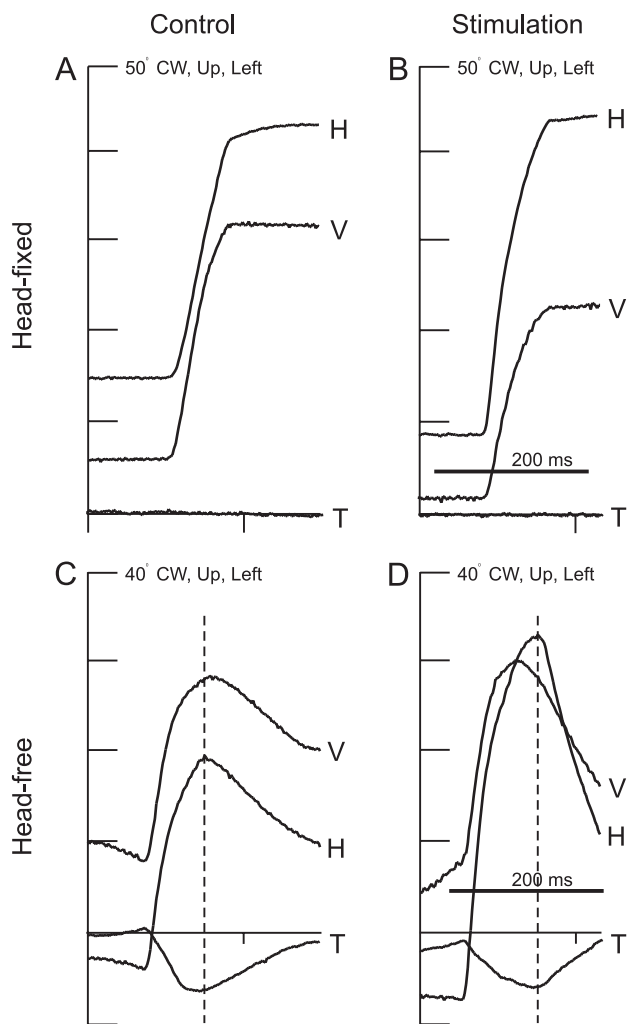


FIG. 9. Eh trajectories during head-fixed vs. -free movements. The 3 components of the Eh (horizontal, H; vertical, V; and torsional, T) are plotted as a function of time in Listing's coordinates. *A* and *B*: with the head fixed, torsion remains in Listing's plane (i.e., plane of 0 torsion) throughout control (*A*) and stimulation-induced (*B*) movements. *C* and *D*: in contrast, with the head free, torsion is driven out of and then back into Listing's plane during either control (*C*) and stimulation-induced movement (*D*). ---, the end of the gaze shift.

Does Eh torsion still remain in Listing's plane throughout the entire trajectory?

Figure 9, *C* and *D*, shows the three components of the Eh during head-free gaze shifts elicited during matched control and stimulation conditions, respectively. In these head-free conditions, the head moved up and to the left (not shown). In both cases, the Eh was also initially displaced up and to the left. But notice that this time the corresponding Eh torsional components did not remain in Listing's plane throughout the entire trajectory. First, Eh torsion appears to be driven out of Listing's plane up to the end of the gaze shift (dashed line), and subsequently comes back into Listing's plane during the VOR-related Eh movement. Thus stimulation of one SC site can produce zero torsion (head-fixed) or a pattern of torsional movement (head-free). But why does the latter occur?

Eye-head coordination

To answer these questions, we first needed to examine these torsional deviations (i.e., bumps) in the control data. Figure

10A depicts five head-free Eh trajectories elicited during random gaze shifts, showing torsional deviations (re: Listing's plane) as a function of time. All the trajectories are aligned on the end of the gaze shift (dashed line), and the five examples are shown to illustrate that Eh torsion is variable across different movements. The part of the trajectory to the left of the dashed line represents the torsion associated with the gaze shift part of the eye movement (when the line of site is realigned), whereas the part of the trajectory to the right of the dashed line shows torsional movement during the VOR-related Eh movement that follows the gaze shift. In each of these traces, torsion appears to be driven out of Listing's plane during the gaze shift and then seems to be brought back into Listing's plane during the VOR movement.

Thus Listing's law is not obeyed *during* these movements. The VOR-related Eh torsion (right of dashed line) violates Listing's law and is unavoidable. This is because the VOR acts to stabilize gaze on a target, and this can only be done by rotating the eye about an equal and opposite axis to that of head rotation. If, during the VOR phase, the head is rotating about an axis with some torsional component, then the eye must also have a torsional component of rotation if the VOR is to be successful. And it is this imposed ocular torsion that drives the eye out of Listing's plane during head-free gaze shifts. To counteract this, an equal but opposite torsional component in the preceding gaze movement (left of dashed line) would cancel the inevitable VOR-induced Eh torsion. Note that the size of these movements vary depending on the size of the torsional head component. In this way, torsion could be minimized at the end of each completed movement, as observed previously in normal behavior (Crawford et al. 1999; Tweed et al. 1998).

To quantify this, we computed the torsional amplitude away from Listing's plane during the gaze shift and plotted it as a function of the torsional amplitude back toward Listing's plane during the subsequent VOR-induced Eh movement. If the Eh is directed in one direction during the gaze shift and then driven in an equal and opposite direction during the ensuing VOR movement, then these two measures should be equal, and a slope of 1 is predicted. Data for *M1* are shown in Fig. 10B and data for *M2* are shown in Fig. 10C along with their slopes and regression coefficients. The computed slopes were quite steep (*M1* = 0.82; *M2* = 0.88); however, they were significantly different from 1 [*M1*, $t(226) = 4.49$, $P < 0.05$; *M2*, $t(319) = 6.20$, $P < 0.05$]. Therefore in control data, Eh torsion was driven out of and back into Listing's plane by nearly equal amounts. We postulate that the remaining accumulated torsion is removed by smaller corrective mechanisms that operate in between gaze shifts (see Fig. 12) as has been shown previously for head-fixed eye movements (Van Opstal et al. 1996).

Does this same pattern also hold for stimulation-induced movements? Figure 10D shows five torsional Eh trajectories that were elicited by SC stimulation. These trajectories are amplitude-matched to those derived from control data in Fig. 10A. Again, the same pattern of increasing (during the gaze shift) and decreasing (during the VOR) torsional movement relative to Listing's plane was observed. Stimulation-induced trajectories with single steps were quantified like the control data in the preceding text for *M1* (Fig. 10E) and *M2* (Fig. 10F). Double- and triple-step gaze shifts could not be similarly quantified as the Eh torsional pattern oscillated several times

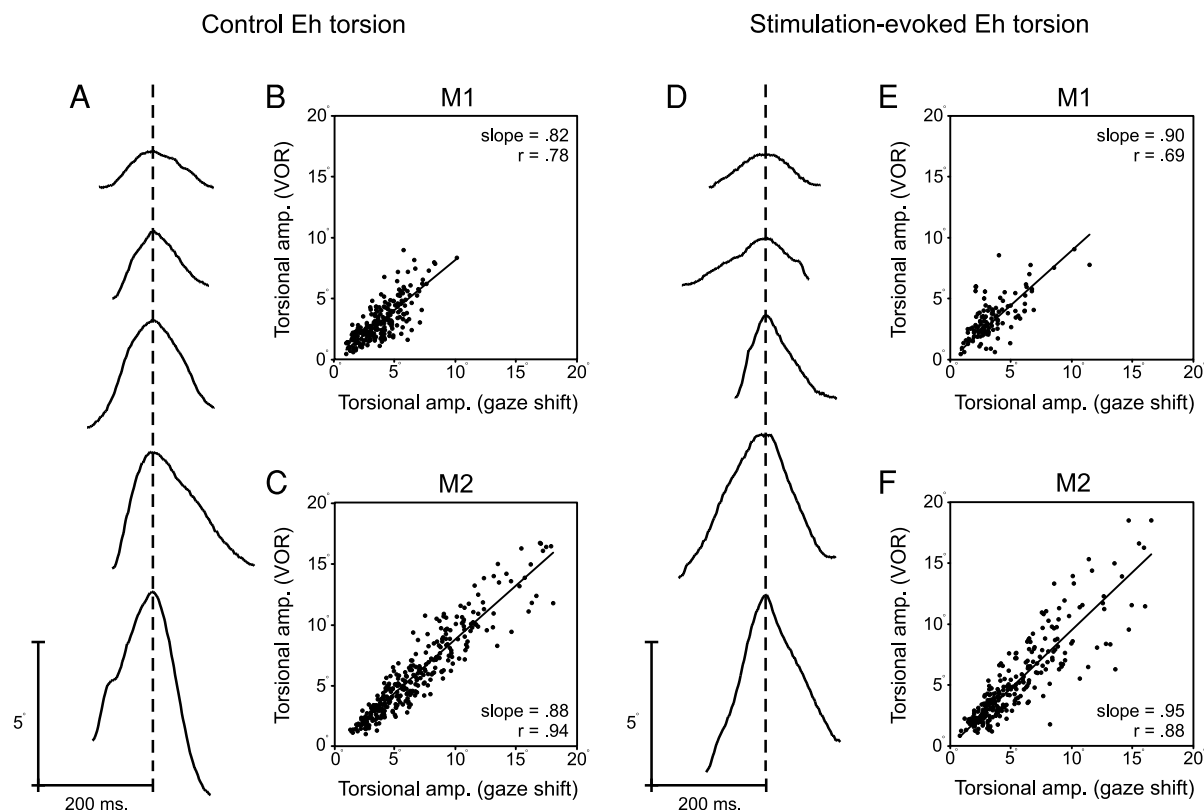


FIG. 10. Torsional pattern of Eh movements during gaze shifts. Five examples of Eh torsional traces are shown for SC control (A) and stimulation-evoked behavior (D). Torsional amplitude increases down each column and corresponding traces in each column are amplitude-matched. The trajectories down each column are aligned (dashed line) at the end of the gaze shift (i.e., when the Es had reached the target, but the Hs had not yet completed its movement). Thus the part of the trace to the left of the dashed line indicates the gaze-shift movement, whereas the part of the trace to the right of the dashed line indicates the VOR-related movement. These torsional “bumps” were quantified by computing the torsional amplitude of the Eh during the gaze shift and VOR portions of control (B and C) and stimulation-induced (E and F) movements for each monkey (M1 and M2). Slopes and correlation coefficients are given in the figure.

during each gaze shift. The data shown are from the dim condition where the slopes were not significantly different from a slope of 1 [M1, $t(126) = 1.73$, $P > 0.05$; M2, $t(285) = 1.79$, $P > 0.05$]. The dark condition showed similar relationships (M1 slope = 0.727, $r = 0.577$; M2 slope = 0.915, $r = 0.717$), but the slopes here were significantly different from 1 [M1, $t(161) = 5.87$, $P < 0.05$; M2, $t(305) = 2.11$, $P < 0.05$]. Because the slopes in the dark condition were nevertheless quite high, we will show that the remaining torsion was corrected via smaller corrective movements before the start of the next gaze shift (see Fig. 12) (Van Opstal et al. 1996).

Therefore even during stimulations, Eh torsion was driven away from Listing’s plane during the gaze shift by a nearly equal and opposite amount as it was during the subsequent VOR-related head movement. Because this stimulation-induced pattern of Eh torsion is similar to that of our controls and as that reported previously for head-free behavior (Crawford et al. 1999), then we propose that the same active anticipatory mechanism found in controls underlies the behavior in SC stimulation data.

But before we continue with this hypothesis, perhaps an alternative interpretation of these data are that they are unusually large torsional transients—i.e., passive movements resulting from pulse-step mismatch (Schnabolk and Raphan 1994; Tweed et al. 1994). Therefore it was important to determine if

these movements were not passive drifts of the Eh out of and back into Listing’s plane. Torsional transients should have time constants equal to that of the plant, which for the torsional dimension have been estimated at 83 ms for extorsion and 210 ms for intorsion (Seidman et al. 1995). However, the average time constant of the torsional component accompanying the gaze shift portion of the stimulation-induced movement was 36.8 ± 9.6 (SE) ms, indicating that these were actively generated movements because their time constants were smaller than those of the plant. Also, the torsional movements that accompanied the VOR phase of our stimulation-induced movements had time constants of 46.4 ± 6.0 ms, again showing neurally produced movements and not simply passive Eh drift.

In addition, to verify that the latter movements were part of a normal 3-D VOR, we compared the axes of rotation of the eye and head during this phase. It is known that during the monkey VOR, the Eh rotates about a 3-D axis that is equal and opposite to that of the head (Crawford and Vilis 1991; Misslisch and Hess 2000). This is done so that gaze can remain stably oriented on the object of interest. In Fig. 11, we plotted Eh (dark) and Hs (light) velocity traces for the three largest movements in Fig. 10A (velocity traces of the smallest 2 movements were too small for visual comparisons). It is evident, in both the behind (*left*) and side (*right*) views that the Es and Hs move in equal and opposite 3-D paths during the latter

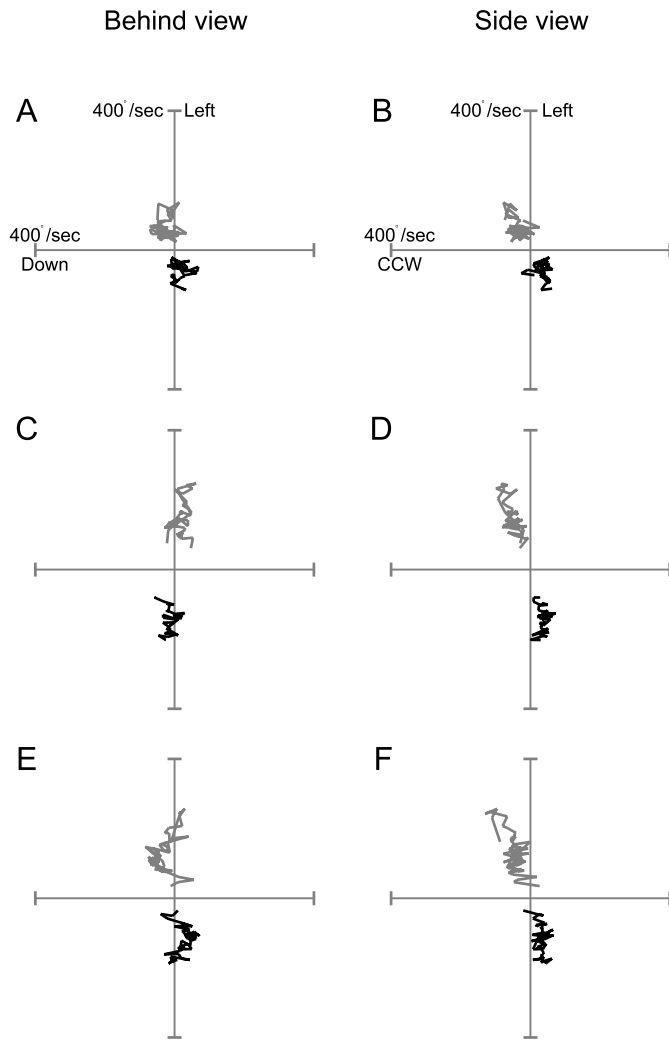


FIG. 11. VOR-related Eh movements. Velocity traces of the Eh (black) and Hs (gray) are plotted in behind (left) and side (right) views. These traces correspond to the last 3 stimulation-induced Eh plots from Fig. 10 (A and B, 3rd trace; C and D, 4th trace; E and F, 5th trace). If these plots of Eh were indeed caused by head-induced VOR, then the velocity traces of the Eh and Hs should appear equal and opposite (in head coordinates). This is because the VOR serves to rotate the Eh in an equal and opposite direction to that of the Hs. In this way, final gaze (i.e., Es) alignment can remain stable while the Hs finishes its stimulation-induced movement.

part of the gaze shift. Thus these movements appear to be nothing other than ordinary VOR movements, resulting in violations of Listing's law which can only be compensated by equal and opposite torsional quick phases if one wants to land in Listing's plane at the end of the gaze shift.

Quantifying intra-gaze shift torsion

To further quantify this torsional "bump" pattern of movements for the Eh, as well as to obtain comparable torsional values for the Hs and Eh, we measured the Tsd at several points during both stimulation-induced and control gaze shifts. Specifically, we examined fixation points (i.e., when the velocity of both the eye and head were <math><10^\circ/s</math>), gaze end points (i.e., when the Es had reached its new gaze position, but the head had not finished its movement), and VOR endpoints (i.e., when the Hs had stopped its movement; see Fig. 1). These

points were chosen because, according to Crawford et al. (1999), it is here that the Eh exhibits its pattern of increasing and subsequent decreasing Tsd during control behavior. The averaged Tsd ($\pm SE$) for both monkeys (M1 and M2), for the Es, Hs, and Eh are shown for control and stimulation-induced data in Fig. 12.

Despite individual differences between M1 and M2, both monkeys show the same trends during control behavior (top). Tsd for the Es, Hs, and Eh is always lowest before the beginning of each movement (i.e., during fixations). As the movement proceeds, the line of sight is displaced from its initial to its final position. At this point (the gaze shift end point), the Tsd in all three variables increases. For the Es and Hs, this increase is still present at the end of the Hs movement (i.e., the VOR end point). It is worth noting that these elevated Tsd levels at the VOR end point are subsequently reduced back down to fixation levels before the next movement (as indicated by the lower Tsd for fixations). This suggests that further small corrective movements during fixations, which follow the rapid head movements, further reduce the Tsd of the Es and Hs.

In contrast, and perhaps most importantly, Tsd of the Eh is significantly reduced back down to near-fixation levels at the end of the head movement. Again, this is the same pattern described previously for normal behavior by Crawford et al. (1999). It may be noted that the final Eh Tsd at the end of the head movement is still not quite as low as the Eh Tsd during fixations. Thus as with the Es and Hs, this Tsd was reduced even further prior to the onset of the next movement through slow corrective mechanisms which we will not address here.

The stimulation data (bottom) was qualitatively and quantitatively similar to the control data. Tsd was always at its lowest

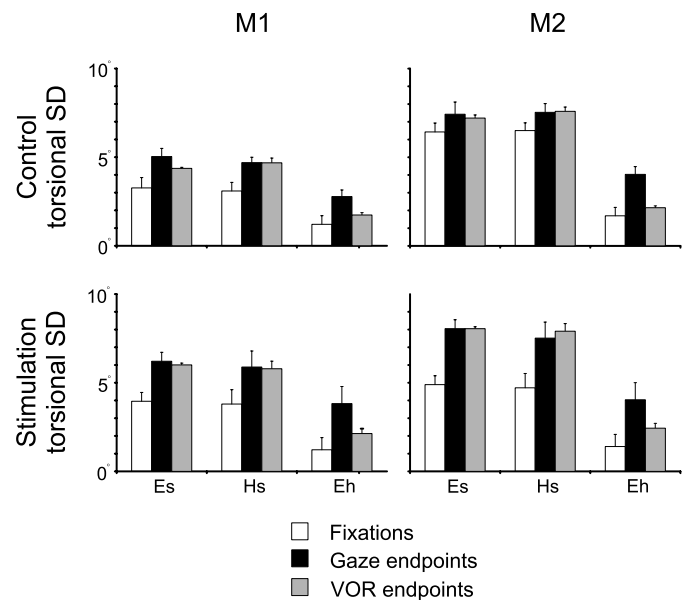


FIG. 12. Torsional SDs (SD) of the Es, Hs, and Eh for normal and SC stimulation-induced behavior. Tsd was measured during fixations (□), gaze shift ends (■), and VOR-related endpoints (▣) for both M1 (left) and M2 (right). In both normal and stimulation conditions, Tsd was always lowest during fixations and subsequently increased during the gaze shift. Tsd of the Eh was always reduced by the end of the VOR-related movement, whereas Tsd of the Es and Hs were reduced by small corrective movements before the next fixation (see text for statistics). Despite some variability across the 2 animals, the Tsd patterns were clear in both conditions, and the amount of Tsd was consistent across the 2 conditions in both M1 and M2.

levels during prestimulation fixations. These levels rose significantly by the end of the gaze shift for the Eh ($P = 0.000$, $M1$; $P = 0.000$, $M2$), Hs ($P = 0.050$, $M1$; $P = 0.000$, $M2$), and Es ($P = 0.022$, $M1$; $P = 0.000$, $M2$). Again, the Hs and Es remained at these elevated levels at the end of the VOR-related movement [Hs ($P = 0.945$, $M1$; $P = 0.648$, $M2$), and Es ($P = 0.858$, $M1$; $P = 0.998$, $M2$)]. And, as in the controls, the Eh returned to near-fixation levels at the end of the head movement ($P = 0.001$, $M1$; $P = 0.000$, $M2$). Finally, the Tsd of all three variables returned to fixation levels before the next movement. Note that these *t*-test values correspond to data in the dim condition, but similar significance values were also found for the dark condition for all comparisons. Overall these data suggest a pattern shared by both control and stimulation data, one that is more complex than a simple restriction to the Donders' surfaces observed during fixations.

DISCUSSION

By electrically microstimulating the SC, a process that reveals the output signal of this structure and not the processing that occurs within or upstream from it, we have shown that the 3-D kinematics of natural movements and those evoked by SC stimulation are highly comparable. First, when 3-D surfaces were fit to the end points of Eh, Hs, and Es movements of both movement types (i.e., stimulation vs. control), the six variables describing the surfaces were statistically identical. Second, measures of Tsd, which indicate how well torsion is constrained about the surface fits, were also statistically identical in both conditions. Third, the mechanism which minimizes Eh torsion (thus maintaining Listing's law) at the end of each gaze shift appears to be the same in SC stimulation data as in normal behavior.

Our previous paper showed that the SC encodes gaze-related activity in retinal coordinates (Klier et al. 2001). Here we demonstrate that the third degree of freedom is only implemented after the SC. In this way, the brain need not concern itself with the torsional kinematics of planning an action until the object of that action has been established. This strategy is extremely efficient because the brain can process a mass of cognitive and perceptual information in its original coordinate system (i.e., relative to the eye) (Henriques et al. 1998).

SC and Donders' law

This study reveals how the 3-D eye-head saccade generator interprets a fixed SC output command. Taken together with previous studies (Freedman and Sparks 1997; Klier et al. 2001), these data suggest that a 2-D oculocentric gaze (Es) signal leaves the SC and is then split into individual commands for the Hs and Eh. The Hs signal appears to take the head along the most direct route to the target (Ceylan et al. 2000; Crawford et al. 1999), while maintaining its final orientations on a Donders' surface (Glenn and Vilis 1992; Radau et al. 1994). However, the Eh command is modified by the addition of torsional components that vary according to the subsequent Hs movement, thereby keeping Es torsional levels compatible with Donders' law.

This study also clarifies the original *head-fixed* SC stimulation findings of Van Opstal et al. (1991) and Hepp et al. (1993). Their observation, that Eh trajectories remain in Listing's

plane, was apparently due to the fact that the head did not contribute any VOR-related torsion. Indeed, our study shows that stimulation of one SC site could produce zero torsion (head-fixed) or various amounts of torsion (head-free) in anticipation of an upcoming head movement. In this way, the downstream structures that interpret the SC command show remarkable context-dependent flexibility.

Thus the oculomotor system is exquisitely tuned to obey Donders' law of the Hs and Eh at the end of each gaze shift, and its implementation serves several purposes. First, it solves the degrees of freedom problem by specifying unique torsional orientations and avoids large torsional Eh positions that would otherwise disturb normal vision (Crawford and Vilis 1991; Misslisch et al. 2001). Some postulate that Donders' strategy is designed to minimize the stretch of eye muscles (Radau et al. 1994), whereas others hypothesize that this strategy optimizes aspects of perception (Glenn and Vilis 1992). But while perceptual consequences are important, Ceylan et al. (2000) showed that motor factors are more important in shaping the moment-to-moment implementation of Donders' law. In any event, these results indicate a close association between Hs and Eh torsion because the former modifies the trajectory of the latter during every gaze shift.

3-D head-free models

To our knowledge, there is only one published model of 3-D eye-head coordination during head-free gaze shifts (Tweed 1997). This model assumes that the SC codes a 2-D eye-centered gaze command, such that all reference frame transformations (i.e., 2- to 3-D transformations) and mechanisms for 3-D eye-head coordination are implemented downstream from the SC. Our previous paper (Klier et al. 2001) supports one of these assumptions—that the SC uses an eye-centered gaze code. But this is separate from the question asked here regarding the implementation of Donders' and Listing's laws because torsion can either be coded in parallel to the SC (in an eye-centered frame) or downstream from it. And both of these schemes can account for the data of Van Opstal et al. (1991) and Hepp et al. (1993). However, the current study confirms the remainder of Tweed's (1997) assumptions—that the transformations proposed in this model can be assigned to brain stem structures downstream from the SC.

Eye-head coordination

The necessity for the eye-head coordination mechanism described here arises from the basic organization of head-free gaze shifts: rapid shifts in gaze that are outlasted by head movements accompanied by the VOR. This system tries to obtain Donders' law at the end of these movements. But typically, during the VOR part of the gaze shift, the Eh is accumulating torsion, potentially as large as $\geq 20^\circ$ (Crawford et al. 1999). One possibility would be to wait for this torsion to occur and then correct it at the end of the gaze shift. But this would disrupt vision at the critical point of foveating the target.

Alternatively, we hypothesize that the brain, having access to information regarding the planned Hs movement and the initial 3-D Eh orientation, anticipates the torsional value to be incurred by the Eh (during the VOR-related Hs movement), and compensates by generating an equal and opposite torsional

signal (during the initial gaze shift). This pattern of eye-head coordination has been predicted in theoretical studies (Tweed 1997) and shown in behavioral studies (Crawford et al. 1999; Tweed et al. 1998). Our results reveal that this mechanism also occurs during SC stimulation and is therefore implemented downstream from the SC.

It has been shown that the SC outputs a 2-D gaze (i.e., Es) command (Freedman and Sparks 1997; Hepp et al. 1993; Klier et al. 2001; Van Opstal et al. 1991). However, the eye-head coordination described in this paper must be implemented on separate Eh and Hs signals. Thus the common gaze signal leaving the SC is probably first decomposed so that the torsional Eh signal can be modified appropriately. Because 3-D kinematic control is most important for specific body parts (i.e., the eyes, the head, etc.), then it is likely that the 2-D gaze is first separated into 2-D Eh and Hs commands, and only afterward is a torsional component added.

Is eye-head coordination neural or mechanical?

Although the implementation of Donders' and Listing's laws must involve mechanical elements, they are fundamentally neural constraints because the Es, Hs, and Eh are capable of rotating torsionally under different circumstances (Crawford and Vilis 1991; Nakayama 1975). It has been suggested that eye muscle insertions on the globe act like "pulleys," which can change muscle pulling direction as a function of eye position (Crawford and Guitton 1997; Demer et al. 1995; Quaia and Optican 1998). This could allow the ocular plant to show more commutative behavior, perhaps simplifying the commands that keep the Eh in Listing's plane. However, this would not help in the current situation where torsional commands are programmed to take the eye out of Listing's plane. Pulley action could also be adjusted via differential commands to the orbital, global, and smooth muscle fibers of the pulleys (Demer et al. 2000), but this seems an unlikely mechanism for the large, rapid, moment-to-moment torsional torques required here for eye-head coordination. In some cases, these corrective movements need to be almost purely torsional (Crawford and Vilis 1991), which is likely beyond the scope of any second-order plant adjustments.

The unique pattern of eye-head coordination described here proves that Eh torsion is not simply maintained at zero but rather increases and decreases according to the magnitude of the head component during a gaze shift. If the plant's goal is to maintain Listing's law or to assign torsion, then each location on the SC should produce only one unique torsional pattern for the Eh. While this theory may have agreed with the head-fixed stimulation data of Van Opstal et al. (1991) and Hepp et al. (1993), it does not agree with our head-free data. We found that each SC site can produce variable amount of torsion depending on parameters such as initial Eh position and the subsequent Hs trajectory. Thus torsion must be constrained neurally, as these types of calculations could not likely be implemented at the level of the eye muscles.

Neural implementation of Donders' and Listing's laws

Assuming that appropriate commands for Donders' and Listing's laws are present at the level of the motoneurons, then where are they implemented? For the Eh, we can now restrict

our search to areas downstream from the SC and upstream from the torsional burst generator (rostral interstitial nucleus of the medial longitudinal fasciculus, riMLF). This is because torsional Eh components are already well defined in the riMLF, where bilaterally symmetric inputs appear to code movements in Listing's plane while asymmetric activity produces abnormal torsion movements (Crawford and Vilis 1992).

One possible structure is the nucleus reticularis tegmentis pontis (NRTP). The NRTP processes signals for all eye movements that obey Listing's law [i.e., saccades (Crandall and Keller 1985), smooth pursuit (Suzuki et al. 1999), and vergence (Gamlin and Clarke 1995)]. Moreover, NRTP activity is correlated with torsional corrective saccades and its inactivation disrupts the maintenance of Listing's law (Van Opstal et al. 1996). This also implicates the cerebellum, which both receives inputs from and projects to the NRTP (Brodal 1980; Gerrits and Voogd 1986).

The central mesencephalic reticular formation (cMRF) may also contribute to the processing of eye-head coordination signals. First, burst-like neurons have been implicated in a feedback circuit to the SC, providing it with information on current eye position and velocity (Waitzman et al. 1996). Second, the cMRF strongly innervates the cervical spinal cord, which in turn innervates the neck muscles that control the head (May et al. 1997). Unfortunately, to date, there have been few cMRF studies measuring head-free behaviors (Waitzman et al. 2001) and none measuring torsional components of eye/head movements. Finally, a distributed circuit involving some or all of these structures may interact to produce these 3-D constraints.

Similar arguments hold for the head-neck system. For example, we recently found that the interstitial nucleus of cajal (INC), the neural integrator for torsional Eh positions, also appears to serve as the neural integrator for torsional Hs positions (Klier et al. 2002). As in oculomotor control, clockwise head movements are coded in the right INC and counterclockwise movement in the left INC. Because these signals appear to encode torsional head position in Fick coordinates (Klier et al. 1999), then bilaterally symmetric inputs to the INC (from the SC) would help to keep the head in its Fick plane (Crawford et al. 1997). Thus we conclude that, during gaze shifts, the 2- to 3-D transformation and implementation of Donders' law for the eyes and head occur between the SC and the premotor nuclei of the brain stem reticular formation.

The authors thank D.Y.P. Henriques, W. P. Medendorp, and M. A. Smith for comments on previous versions of this manuscript.

E. M. Klier was supported by Canadian National Sciences and Engineering Research Council and Ontario Graduate Scholarships. J. D. Crawford holds a Canadian Institutes of Health Research operating grant and is a Canada Research Chair.

REFERENCES

- Bernstein N.** *The Coordination and Regulation of Movements*. Oxford: Pergamon, 1967.
- Brodal P.** The projection from the nucleus reticularis tegmenti pontis to the cerebellum in the rhesus monkey. *Exp Brain Res* 38: 29–36, 1980.
- Ceylan MZ, Henriques DYP, Tweed DB, and Crawford JD.** Task-dependent constraints in motor control: pinhole goggles make the head move like an eye. *J Neurosci* 20: 2719–2730, 2000.
- Crandall WF and Keller EL.** Visual and oculomotor signals in nucleus reticularis tegmenti pontis in alert monkey. *J Neurophysiol* 54: 1326–1345, 1985.

- Crawford JD, Cadera W, and Vilis T.** Generation of torsional and vertical eye position signals by the Interstitial Nucleus of Cajal. *Science* 252: 1551–1553, 1991.
- Crawford JD, Ceylan MZ, Klier EM, and Guitton D.** Three-dimensional eye-head coordination during gaze saccades in the primate. *J Neurophysiol* 81: 1760–1782, 1999.
- Crawford JD and Guitton D.** Visual-motor transformations required for accurate and kinematically correct saccades. *J Neurophysiol* 78: 1447–1467, 1997.
- Crawford JD and Vilis T.** Axes of eye rotation and Listing's law during rotations of the head. *J Neurophysiol* 65: 407–423, 1991.
- Crawford JD and Vilis T.** Symmetry of oculomotor burst neuron coordinates about Listing's plane. *J Neurophysiol* 68: 432–448, 1992.
- Crawford JD and Vilis T.** How do motor systems deal with the problems of controlling three-dimensional rotations? *J Motor Behav* 27: 89–99, 1995.
- Crawford JD, Vilis T, and Guitton D.** Neural coordinate systems for head-fixed and head-free gaze shifts. In: *Three-Dimensional Kinematics of Eye, Head, and Limb Movements*, edited by Fetter M, Haslwanter T, Misslisch H, and Tweed D. Amsterdam: Harwood Academic, 1997, p. 43–56.
- Demer JL, Miller JM, Poukens V, Vinters HV, and Glasgow BJ.** Evidence for fibromuscular pulleys of the recti extraocular muscles. *Invest Ophthalmol Vis Sci* 36: 1125–1136, 1995.
- Demer JL, Oh SY, and Poukens V.** Evidence for active control of rectus extraocular muscle pulleys. *Invest Ophthalmol Vis Sci* 41: 1280–1290, 2000.
- Donders FC.** Beitrag zur Lehre von den Bewegungen des menschlichen Auges. *Hollandische Beiträge Anat Physiol Wiss* 1: 105–145, 1848.
- Ferman L, Collewijn H, and Van Den Berg AV.** A direct test of Listing's law. I. Human ocular torsion measured in static tertiary positions. *Vision Res* 27: 929–938, 1987.
- Fick A.** Die Bewegungen des menschlichen Augapfels. *Z Rationelle Med* 4: 101–128, 1854.
- Freedman EG and Sparks DL.** Activity of cells in the deeper layers of the superior colliculus of the rhesus monkey: evidence for a gaze displacement command. *J Neurophysiol* 78: 1669–1690, 1997.
- Freedman EG, Stanford TR, and Sparks DL.** Combined eye-head gaze shifts produced by electrical stimulation of the superior colliculus in rhesus monkeys. *J Neurophysiol* 76: 927–952, 1996.
- Gamlin PD and Clarke RJ.** Single-unit activity in the primate nucleus reticularis tegmenti pontis related to vergence and ocular accommodation. *J Neurophysiol* 73: 2115–2119, 1995.
- Gerrits NM and Voogd J.** The nucleus reticularis tegmenti pontis and the adjacent rostral paramedian pontine reticular formation: differential projections to the cerebellum and the caudal brain stem. *Exp Brain Res* 62: 29–45, 1986.
- Glenn B and Vilis V.** Violations of Listing's law after large eye and head gaze shifts. *J Neurophysiol* 68: 309–317, 1992.
- Guitton D.** Control of eye-head coordination during orienting gaze shifts. *Trends Neurosci* 15: 174–179, 1992.
- Guitton D, Munoz DP, and Galiana HL.** Gaze control in the cat: studies and modeling of the coupling between orienting eye and head movements in different behavioral tasks. *J Neurophysiol* 64: 509–531, 1990.
- Guitton D and Volle M.** Gaze control in humans: eye-head coordination during orienting movements to targets within and beyond the oculomotor range. *J Neurophysiol* 58: 427–459, 1987.
- Helmholtz H.** *Treatise on Physiological Optics* [English translation], translated by Southall JPC. Rochester, NY: Opt Soc Am, 1867.
- Henriques DYP, Klier EM, Smith MA, Lowy D, and Crawford JD.** Gaze centered remapping of remembered visual space in an open-loop pointing task. *J Neurosci* 18: 1583–1594, 1998.
- Hepp K, van Opstal AJ, Straumann D, Hess BJM, and Henn V.** Monkey superior colliculus represents rapid eye movements in a two-dimensional motor map. *J Neurophysiol* 69: 965–979, 1993.
- Klier EM, Wang H, Constantin AG, and Crawford JD.** The primate midbrain possesses a neural integrator for torsional and vertical head posture. *Science* 295: 1314–1317, 2002.
- Klier EM, Wang H, and Crawford JD.** Stimulation of the interstitial nucleus of Cajal (INC) produces torsional and vertical head rotations in Fick coordinates. *Soc Neurosci Abstr* 25: 50, 1999.
- Klier EM, Wang H, and Crawford JD.** The superior colliculus encodes gaze commands in retinal coordinates. *Nat Neurosci* 4: 627–632, 2001.
- May PJ, Warren S, and Chen BZ.** Pathways for tectal control of vertical eye and head movements. *Soc Neurosci Abstr* 23: 842, 1997.
- Medendorp WP, Melis BJM, Gielen CCAM, and Van Gisbergen JAM.** Off-centric rotation axes in natural head movements: implications for vestibular reafference and kinematic redundancy. *J Neurophysiol* 79: 2025–2039, 1998.
- Misslisch H and Hess BJ.** Three-dimensional vestibuloocular reflex of the monkey: optimal retinal image stabilization versus Listing's law. *J Neurophysiol* 83: 3264–3276, 2000.
- Misslisch H, Tweed D, and Hess BJ.** Stereopsis outweighs gravity in the control of the eyes. *J Neurosci* 21: RC126, 2001.
- Misslisch H, Tweed D, and Vilis T.** Neural constraints on eye motion in human eye-head saccades. *J Neurophysiol* 79: 859–869, 1998.
- Munoz DP and Wurtz RH.** Saccade related activity in monkey superior colliculus. II. Spread of activity during saccades. *J Neurophysiol* 73: 2334–2348, 1995.
- Nakayama K.** Kinematics of normal and strabismic eyes. In: *Vergence Eye Movements: Basic and Clinical Aspects*, edited by Schor CM and Ciuffreda KJ. Boston, MA: Butterworths, 1975, p. 288–321.
- Newlands SD, Hesse SV, Haque A, and Angelaki DE.** Head unrestrained horizontal gaze shifts after unilateral labyrinthectomy in the rhesus monkey. *Exp Brain Res* 140: 25–33, 2001.
- Phillips JO, Ling L, Fuchs AF, Siebold C, and Plorde JJ.** Rapid horizontal gaze movement in the monkey. *J Neurophysiol* 73: 1632–1652, 1995.
- Pierrot-Desilligny C, Rivaud S, Gaymard B, Muri R, and Vermersch AI.** Cortical control of saccades. *Ann Neurol* 37: 557–567, 1995.
- Quaia C and Optican LM.** Commutative saccadic generator is sufficient to control a 3-D ocular plant with pulleys. *J Neurophysiol* 79: 3197–3215, 1998.
- Radau P, Tweed D, and Vilis T.** Three-dimensional eye, head and chest orientations following large gaze shifts and the underlying neural strategies. *J Neurophysiol* 72: 2840–2852, 1994.
- Richmond FJR and Vidal PP.** The motor system: joints and muscles of the neck. In: *Control of Head Movement*, edited by Peterson BW and Richmond FJR. New York: Oxford Univ. Press, 1998, p. 1–21.
- Roucoux A, Guitton D, and Crommelinck M.** Stimulation of the superior colliculus in the alert cat. II. Eye and head movements evoked when the head is unrestrained. *Exp Brain Res* 39: 75–85, 1980.
- Schnabolk C and Raphan T.** Modeling three-dimensional velocity-to-position transformation in oculomotor control. *J Neurophysiol* 71: 623–638, 1994.
- Schreiber K, Crawford JD, Fetter M, and Tweed D.** The motor side of depth vision. *Nature* 410: 819–822, 2001.
- Seidman SH, Leigh RJ, Tomsak RL, Grant MP, and Dell'Osso LF.** Dynamic properties of the human vestibulo-ocular reflex during head rotations in roll. *Vision Res* 35: 679–689, 1995.
- Suzuki DA, Yamada T, Hoedema R, and Yee RD.** Smooth-pursuit eye-movement deficits with chemical lesions in macaque nucleus reticularis tegmenti pontis. *J Neurophysiol* 82: 1178–1186, 1999.
- Theeuwes M, Miller LE, and Gielen CCAM.** Is the orientation of head and arm coupled during pointing movements? *J Mot Behav* 25: 242–250, 1993.
- Tomlinson RD.** Combined eye-head gaze shifts in the primate. III. Contributions to the accuracy of gaze saccades. *J Neurophysiol* 64: 1873–1891, 1990.
- Turvey MT.** Coordination. *Am Psychol* 45: 938–953, 1990.
- Tweed D.** Three-dimensional model of the human eye-head saccadic system. *J Neurophysiol* 77: 654–666, 1997.
- Tweed D, Cadera W, and Vilis T.** Computing three-dimensional eye position quaternions and eye velocity from search coil signals. *Vision Res* 30: 97–110, 1990.
- Tweed D, Glenn B, and Vilis T.** Eye-head coordination during large gaze shifts. *J Neurophysiol* 73: 766–779, 1995.
- Tweed D, Haslwanter T, and Fetter M.** Optimizing gaze control in three dimensions. *Science* 281: 1363–1366, 1998.
- Tweed D, Misslisch H, and Fetter M.** Testing models of oculomotor velocity-to-position transformation. *J Neurophysiol* 72: 1425–1429, 1994.
- Tweed D and Vilis T.** Geometric relations of eye position and velocity vectors during saccades. *Vision Res* 30: 111–127, 1990.
- Van Opstal AJ, Hepp K, Hess BJM, Straumann D, and Henn V.** Two-rather than three-dimensional representation of saccades in monkey superior colliculus. *Science* 252: 1313–1315, 1991.
- Van Opstal AJ, Hepp K, Suzuki Y, and Henn V.** Role of monkey nucleus reticularis tegmenti pontis in the stabilization of Listing's plane. *J Neurosci* 16: 7284–7296, 1996.
- Waitzman DM, Pathmanathan J, Cullen KE, Presnell R, May JP, and Madara J.** Signals related to movements of the head and eyes in the mesencephalic reticular formation (MRF) of primate. *Soc Neurosci Abstr* 27: 405.14, 2001.
- Waitzman DM, Silakov VL, and Cohen B.** Central mesencephalic reticular formation (cMRF) neurons discharging before and during eye movements. *J Neurophysiol* 75: 1546–1572, 1996.
- Westheimer G.** Kinematics of the eye. *J Opt Soc Am* 47: 967–974, 1957.